Projected water table depth changes of the world's major groundwater basins

Maya Costantini[1], Jeanne Colin[1], Bertrand Decharme[1]

[1]Centre National de Recherches Météorologiques (CNRM), Météo-France/CNRS, Toulouse, France

Key Points:

- The impact of climate change on water table depth in the world's major groundwater basins is assessed using CMIP6 global simulations.
- Projections run with four SSP scenarios show a global rising of groundwater by 2100, with the occurrence of a depletion in numerous regions.
- In 2100, 31% to 43% of the world's population could face water scarcity issues or flood risks worsened by these water table depth changes.

Corresponding author: Maya Costantini, `maya.costantini@meteo.fr`

Abstract

As groundwater found in aquifers is the main reservoir of freshwater for human activity, knowledge of the future response of groundwater to climate change is key for improving water management adaptation plans. We analyse the climate-driven evolution of future levels of unconfined aquifers in the 218 world's major groundwater basins in global climate simulations following the latest IPCC scenarios, run with models able to capture feedbacks among climate, land use and groundwater. We find a rising of groundwater levels on global average, which is consistent with the projected global intensification of precipitation. However, the evolution of water table depths is not spatially uniform and presents large regional disparities. Depending on the scenario, we find a statistically significant rise (respectively a depletion) of groundwater levels in 2100 over 40[34-47]% to 52[50-54]% (respectively 20[19-24]% to 26[25-29]%) of the area covered by the 218 world's major groundwater basins. Using spatializaed projections of population in 2100, we estimate that 31[29-36]% to 43[42-44]% of the world's population could be affected by these groundwater changes, facing either water scarcity issues, or increased risks of flooding. As the climate models we used do not represent human groundwater withdrawals (irrigation as well as domestic and industrial uses), we also use FAO maps of present-day irrigated areas and projections of population to identify regions where groundwater withdrawals could exacerbate the projected depletion, or even reverse a projected rise into a depletion.

1 Introduction

Groundwater, stored in permeable geological structures (aquifers), constitutes the largest unfrozen reserve of freshwater on Earth. It amounts to approximately 35% of human fresh water withdrawals (Doll et al., 2012) and sustains ecosystems by supplying baseflow during dry periods. The recharge of aquifers stems mainly from rainfall, melted snow, and water exchanges with inland water bodies. Conversely, groundwater sustains these bodies of water and is the main driver of river flow. To a lesser extent, it also contributes to evapotranspiration in groundwater-dependent ecosystems. In addition to these natural water fluxes, pumping and soil infiltration of irrigation water also affect groundwater levels. The evolution of groundwater resources with climate change is therefore of great importance for both humankind and natural ecosystems.

As climate change modify the natural hydrological cycle as well as human water use and demand, it also affect groundwater resources (Green et al., 2011; R. G. Taylor et al., 2013; Wada, 2016; Scanlon et al., 2012; IPCC, 2021c). Over the past decade, studies exploring the impact of future climate change on groundwater have relied on hydrological models driven by atmospheric forcing or estimated recharge. Until the recent work of Wu et al. (2020), who used a fully coupled global climate model, studies exploring the impacts of future climate change on groundwater have relied on hydrological models driven by atmospheric forcings or estimated recharges. Few of these studies are global (Wada et al., 2012; Reinecke et al., 2021). In most cases, the spatial scale is limited to a given set of watershed or a single region (Meixner et al., 2016; Maxwell & Kollet, 2008; Condon et al., 2020; Amanambu et al., 2020). These global and regional studies give valuable insights regarding the future of groundwater resources, but regardless of their scale, they can not take into account the groundwater-climate feedbacks because of their modelling framework. A number of studies have shown that including groundwater in a coupled surface-atmosphere model leads to an increase of evapotranspiration, which can impact near-surface temperature and precipitation (e.g. Anyah et al. (2008); Larsen et al. (2016); Wang et al. (2018)). Without these feedbacks, the response of groundwater to climate change may be biased (Maxwell & Kollet, 2008; Meixner et al., 2016), and the future long-term evolution of the land surface hydrology can be misleading (Boe, 2021).

Over the past few years, a number of authors have recommended the inclusion of a representation of groundwater in Earth system models and global climate models(Clark et al., 2015; Fan et al., 2019; Boe, 2021; Gleeson et al., 2021), and some of them have argued that these integrated models would ultimately help to assess the future effects of climate change on groundwater(Fan et al., 2019; Gleeson et al., 2021). Taking up this suggestion, Wu et al. (2020) considered an ensemble of future global simulations following the old business-as-usual RCP8.5 scenario (designed for the fifth phase of the Coupled Model Intercomparison Project CMIP5 (K. E. Taylor et al., 2012)), performed with the Community Earth System Model version 4.0 (Kay et al., 2015) which includes a simple parameterization of aquifers. The authors analysed the future evolution of groundwater storage in this ensemble of projections, but they limited their assessment to 7 key mid-latitudes aquifers, thus failing to provide a worldwide picture of the global changes.

In this present study, we look to go beyond the work of Wu et al. (2020) by providing a wider scale analysis of future groundwater levels using more recent global climate simulations. To do so, we consider the future climate-driven evolution of the 218 world's major groundwater basins which cover 43% of the global land surface (without Antarctica and Greenland) and under four of the up-to-date greenhouse gas concentration pathways scenarios (SSP126, SSP245, SSP370 and SSP585) (O'Neill et al., 2017). The simulations were performed at the French National Center for Meteorological Research (CNRM in french), for the sixth phase of the Coupled Model Intercomparison Project (CMIP6) (Eyring et al., 2016) with our two fully coupled climate models CNRM-CM6-1 (Voldoire et al., 2019) and CNRM-ESM2-1 (Seferian et al., 2019). Both models include a hydrogeological representation of unconfined aquifer processes in the world's major groundwater basins (Decharme et al., 2019; Vergnes & Decharme, 2012). They simulate the evolution of the Water Table Depth (WTD), defined as the depth of the piezometric head in each aquifer, using a two-dimensional diffusive scheme of the groundwater flows also accounting for two-way water exchanges with the river and the unsaturated soil column. This two-way coupling allows the CNRM models to capture groundwater-climate feedbacks, and CNRM-ESM2-1 also accounts for land-use changes feedbacks.

The recently issued IPCC Sixth Assessment Report (AR6) (IPCC, 2022a) pointed out the necessity to include such feedbacks in projections of future groundwater resources. With the inclusion of these processes in the CNRM models, the present study contributes to further narrow one of the knowledge gaps identified in the AR6 (IPCC, 2022a). However, human groundwater withdrawals and irrigation are not simulated in the CNRM models, as is also the case for most of the models used in the previously mentioned studies. Therefore, our analysis only considers the "natural" part of the climate change-induced changes of water table depths. .

Hereafter, the evolution of WTD is analysed over the 1850-2100 period using CMIP6 simulations run with the CNRM models. The results are put in perspective with a multi-model analysis of the precipitation and evapotranspiration changes simulated by 18 other state-of-the-art global climate models which contributed to CMIP6. Finally, we discuss the foreseeable impacts of the projected evolution of groundwater levels on the human water need in 2100, and vice versa.

2 Materials and Methods

2.1 CNRM models

The global climate model CNRM-CM6-1 (`http://www.umr-cnrm.fr/cmip6/spip.php?article11`) and the Earth system model CNRM-ESM2-1 (`http://www.umr-cnrm.fr/cmip6/spip.php?article10`) are both two global fully coupled atmosphere-ocean-surface

general circulation models of the CNRM. They are part of the models engaged in CMIP6 to contribute to the AR6 (Eyring et al., 2016; IPCC, 2021a). These models are run at a resolution of approximately 1.5° and based on the same core of components. CNRM-CM6-1 simulates the main physical processes in the ocean, the sea ice, the land surface and the atmosphere (Voldoire et al., 2019). Using the same physics, CNRM-ESM2-1 represents in addition the global carbon cycle including carbon cycling in vegetation. Leaf level photosynthesis, plant respiration, stomatal conductance, and plant biomass are explicitly computed by the model. Leaf phenology results directly from the simulated carbon balance of the canopy (Delire et al., 2020). This allows to represent the physiological effects of CO_2 on plant transpiration and growth (increased water use efficiency and fertilisation effect). CNRM-ESM2-1 also accounts for land-use-land-cover change scenarios derived from the Land Use Harmonized version 2 release LUH2 (Hurtt et al., 2020) for CMIP6 and includes an interactive atmospheric chemistry scheme and an interactive tropospheric aerosols scheme (Seferian et al., 2019).

In these two climate models, the ISBA-CTRIP (Decharme et al., 2019) (Interaction-Soil-Biosphere-Atmosphere - CNRM version of the Total Runoff Integrating Pathways) land surface system provides a physical and realistic representation of the continental hydrology (`http://www.umr-cnrm.fr/spip.php?article1092\&lang=en`). ISBA uses multilayer schemes for both the soil and the snowpack to calculate the time evolution of the water and energy budgets at the land surface and to provide water flow to CTRIP. In this way, CTRIP which simulates inundation dynamic, groundwater processes and river discharges in the ocean. Because of the coarse resolution of the model (0.5°), only the 218 world's largest unconfined aquifer basins with diffusive groundwater movements are represented for the moment (Vergnes & Decharme, 2012; Vergnes et al., 2012). More complex aquifer systems like confined, karstic, orogenic and localized shallow aquifers remain difficult to simulate at the global scale due to the lack of precise global parameter database. The hydrogeological modelling of groundwater dynamics relies on a two-dimensional one-layer diffusive widespread unconfined aquifer scheme (Vergnes et al., 2012) based on the well-known MODCOU hydrogeological model (Vergnes, May 2014; Ledoux et al., 1989). This scheme computes the WTD in aquifers according to the lateral groundwater fluxes, the two-way water exchanges with the rivers (Vergnes & Decharme, 2012; Vergnes et al., 2012) and the unsaturated soil (Decharme et al., 2019; Vergnes J.P., Decharme B, 2014). Groundwater basins boundaries and their hydrogeological parameters were estimated using global maps of groundwater resources and topological, lithological and geological data sets (Vergnes & Decharme, 2012). Groundwater basins have been delimited using the global map of the groundwater resources of the world from the Worldwide Hydrogeological Mapping and Assessment Programme (WHYMAP), the hydrogeological map over the United States from the U.S. Geological Survey (USGS) and the global map of lithology (Durr et al., 2005). This last map also allows one to determine the transmissivity and the effective porosity in each aquifer basin (Vergnes & Decharme, 2012; Decharme et al., 2019).

Groundwater processes as well as other hydrological features were validated thoroughly during the last decade in ISBA-CTRIP on a regional and global scale. These evaluations were performed specifically by comparing model results to in-situ measurements of the piezometric head, the GRACE terrestrial water storage estimates and a large set of in-situ river discharges measurements in forced land surface applications (Decharme et al., 2019; Vergnes & Decharme, 2012; Vergnes et al., 2012; Vergnes J.P., Decharme B, 2014) as well as in our fully-coupled climate models (Voldoire et al., 2019; Roehrig et al., 2020). Finally, it was thanks to this evaluation work that the ISBA-CTRIP land surface system was used in many global hydrological applications, some of which highlight important results regarding global hydrology and climate change (Padron et al., 2020; Cazenave et al., 2014; Douville et al., 2013).

In this study, we only consider the WTD which are shallower than 100 m (WTD$< 100m$) over $1985 - 2014$ in the historical CMIP6 experiment (present-day climate). In deeper aquifers, we assume that groundwater is too disconnected from the surface to be significantly impacted by climate change at the time scales we consider (less than 250 years). This is especially true over hyper-arid regions (e.g. in the Sahara desert) where fossil aquifers were recharged by precipitation during paleoclimatic periods (R. G. Taylor et al., 2013; Scanlon et al., 2006; Alley et al., 2002). The current annual precipitation rates here are extremely weak, which limits the groundwater recharge and thus constrains WTD to very deep levels.

2.2 CMIP6 Experiments and Data Post-processing

Our analysis of the water table depth changes is based on the results of CMIP6 simulations run with the CNRM models. The multi-model analysis includes the results of CMIP6 simulations run with the 18 models of the CMIP6 panel which had published the variables of interest (see next subsection) at the time of our analysis (see Table 1). For the past and present-day climate ($1850 - 2014$) we use simulations run for the historical experiment, which is part of the CMIP6 core experiments (Eyring et al., 2016). For the future period ($2015 - 2100$), we use simulations run for the ScenarioMIP experiments (O'Neill et al., 2016, 2017; Meinshausen et al., 2017). We consider four scenarios, based on different Shared Socioeconomic Pathways (SSP) and different levels of radiative forcing (increase of the atmosphere's radiative balance (in $W.m^{-2}$) between 1850 and 2100) : SSP126, SSP145, SSP370, SSP585. To put it simply, the SSP126 scenario is the optimistic one. It is defined by a sustainable societal development, with a relatively low radiative forcing. The SSP245 scenario is a middle-of-the-road pathway. It depicts a world where the socioeconomic trends do not deviate too much from the historical period patterns, with an intermediate radiative forcing. The SSP370 scenario displays regional rivalries and a higher radiative forcing. The SSP585 scenario in the worst case scenario, with a strong fossil-fueled development and a subsequently high radiative forcing.

For each experiment (historical or scenarios), models run an ensemble of simulations, composed of several members. These ensembles allows to sample the climate internal variability and thus provides a better assessment the models' response to the evolution of climate forcings (the more members, the better). We used all the available members at the time of our analysis (see Table 1). The variables we considered are the Water Table Depth (WTD), precipitation (PR) and evapotranspiration ($EVSPSBL$). As the two CNRM climate models provide similar results for the variables of interest, their data were processed jointly. The same weight was given to CNRM-CM6-1 and CNRM-ESM2-1 by first computing the ensemble mean of each model (average of all members) for each variable and each experiment, and then averaging the two ensemble means. For the multi-model analysis of the 18 other state-of-the-art CMIP6 models we considered, we also computed the ensemble means of each model, and then we averaged these ensemble means. All the variables computed by the different CMIP6 models were regridded on the 0.5° regular grid over which WTD is computed in the CNRM models. The interpolation was done using a first order conservative remapping provided by the Climate Data Operator (CDO: http://www.idris.fr/media/ada/cdo.pdf). The interpolation was performed on the ensemble means of each model, as were any further statistical computations (time series, averages over time periods, percentages of change, etc.).

Table 1. Models used and number of members for each model

Global Climate Model	Number of members (historical)	Number of members (SSPs)
$CNRM/CNRM - CM6 - 1$	30	6
$CNRM/CNRM - EMS2 - 1$	11	5
$BCC/BCC - CSM2 - MR$	3	1
$CAS/FGOALS - f3 - L$	3	3
$CAS/FGOALS - g3$	6	4
$CCCma/CanESM5 - CanOE$	3	3
$CCCma/CanESM5$	40	25
$CSIRO/ACCESS - ESM1 - 5$	10	3
$INM/INM - CM4 - 8$	1	1
$INM/INM - CM5 - 0$	10	1
$IPSL/IPSL - CM6A - LR$	32	6
$MIROC/MIROC6$	50	50
$MIROC/MIROC - ES2L$	10	1
$MOHC/UKESM1 - 0 - LL$	11	5
$NASA - GISS/GISS - E2 - 1 - G$	10	1
$NCAR/CESM2$	11	5
$NCAR/CESM2 - WACCM$	3	5
$NIMS - KMA/KAGE - 1 - 0 - G$	3	3
$NOAA - GFDL/GFDL - ESM4$	2	1
$UA/MCM - UA - 1 - 0$	1	1

The statistical significance of field differences on maps computed using the False De-
tection Rate (FDR) test(Wilks, 2006, 2016). The FDR test is based on a Student test for
the computation of P-values at each grid point. To determine the significance, P-values
are compared to a threshold which depends on the series of P-values (for every grid point).
This test allows to reduce the rate of false significance, which can be rather high for auto-
correlated fields such as climate variables(Wilks, 2006, 2016). In our case, it gives a better
confidence on the fact that the changes we analyze are truly due to climate change rather
than stemming from internal variability. In addition, to provide confidence intervals on the
fraction of surface impacted by significant changes of water table depth, we used a bootstrap
method. We performed a resampling of the 11 members for each scenario and for the 41 his-
torical members. The FDR test of significance was then computed for each of the bootstrap
1000 samples. The confidence intervals we provide correspond to the 5th and 95th quantiles
of the distribution we obtain with the bootstrap resampling, noted [5th-95th] hereafter.

2.3 Future Population Density Projections

The evolution of population density (people per km^2) is derived from the projection
of population density by countries(KC & Lutz, 2017) conducted for CMIP6 and with the
population density in 2015 at 0.5° provided by the SocioEconomic Data and Applications
Center(SEDAC, 2018). For each country, the percentage of change in population density is
computed between 2015 (see Supporting Information Fig.S1) and 2100 according to CMIP6
projections for each SSP scenario (see Supporting Information Fig.S2). This percentage is
then applied to the population density at 0.5° in 2015 provided by the SEDAC. These global
maps of the world's population in 2100 are used to discuss the possible human impacts of
the projected WTD changes. This information is also used to determine in which regions
our results on WTD changes are likely to be biased by the lack of human groundwater
withdrawals in the CNRM models, and in which way this supposed bias might affect our

results.

2.4 Present-day Irrigation Data

Part of the analysis of our results also refers to maps of areas currently equipped for irrigation in each of the CNRM models grid cells. They are derived from Siebert et al. (2010) using the FAO (Food and Agriculture Organization of the United Nations) data. The two global maps we used provide the percentage of areas equipped for irrigation and the percentage of irrigated areas serviced by groundwater, at a resolution of 5 arc minutes. The two FAO maps was simply interpolated at the 0.5° resolution over which WTD is computed in the CNRM models. And we combined these two maps to compute the percentages of area equipped for groundwater. These data are used to further discuss the possible influence of groundwater withdrawals on our results.

3 Results

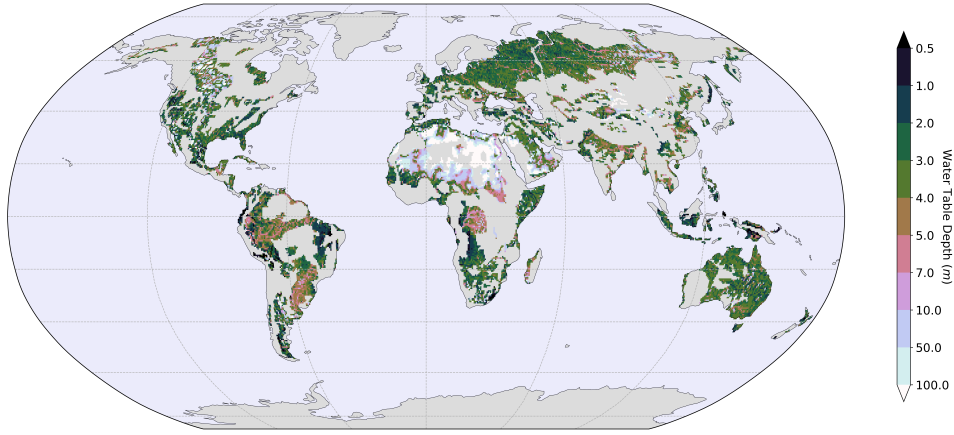### 3.1 Current status and projected groundwater levels

Figure 1. Global distribution of the mean WTD simulated by the CNRM global climate models in the 218 world's major groundwater basins over the present-day period (1985 − 2014) in the historical experiment.

The current status of the world's major groundwater basins simulated by the CNRM models is shown in Fig.1. 40% of the global land area presents a WTD which is shallower than 100 m and 36% of the land area presents WTD between 1 and 10 m. This is consistent with estimates from the high resolution observation-driven model of Fan et al. (2013) based on observations made over the last 60 years (see Supplementary Material in Fan et al. (2013)), where around 38% of the WTD are comprised between 1 and 10 m.

In agreement with recent observational studies(IPCC, 2021b), the globally yearly averaged WTD simulated by the CNRM models shows a slight rise over the 1960 to 2014 period in the historical experiment (Fig.2.A). Following our model estimates, global WTD should continue to rise with climate change in all future scenarios, at least until 2100 (i.e. the end

of the scenarios). The higher the radiative forcing associated to SSP scenarios, the stronger the trend of WTD. The AR6 indicates that the global mean annual precipitation over land is also projected to increase until 2100, in all scenarios(IPCC, 2021c). Precipitation simulated by CNRM models follow the same behavior (Fig.2.B). Overall, the variations of the simulated global WTD follow those of precipitation, except over the $1950 - 1970$ period at a first glance. During this period, the global mean annual precipitation drops because of an increase in sulfur emissions in the atmosphere(Wild, 2012). This is not followed by a decrease of the global mean WTD, even if this decrease is simulated over several regions such as that of south and southeast Asia (not shown). However, the long-term evolution of the two variables are highly correlated, with a R-squared of 0.957 between the 5-yr running means of global WTD and precipitation (not shown).
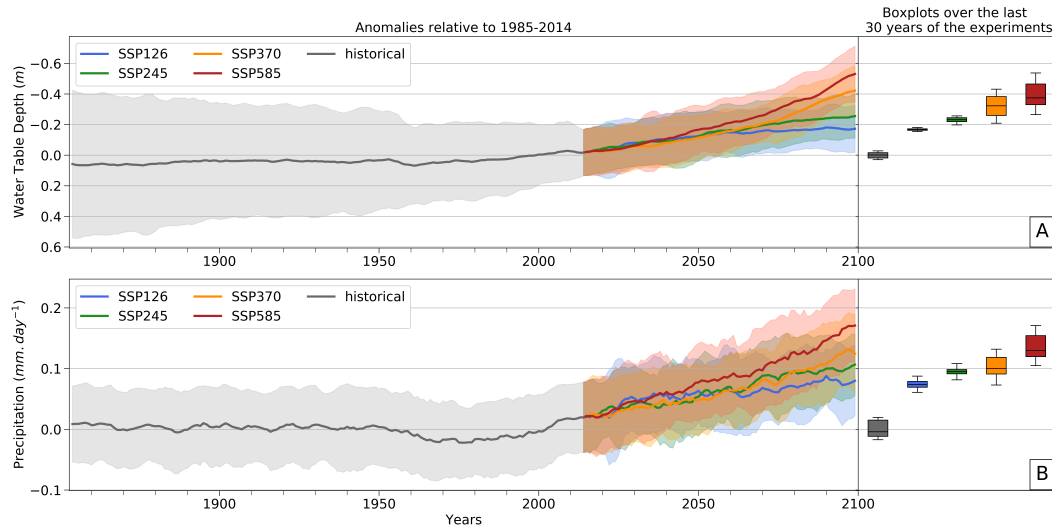

Figure 2. Time series $(1850-2100)$ of the 5-year running average of global mean WTD anomalies (panel **A**) and precipitation over land anomalies (panel **B**), relative to their global average in present-day climate $(1985 - 2014$ period of the historical experiment), according to all scenarios. The shading areas around the global means represent the inter-member spread (± 1.64 inter-member variance) of each experiment. Boxplots further reflect the inter-member distribution of the last 30 years of the historical experiment $(1985-2014)$ and of each scenario $(2071-2100)$. On the boxplots, the vertical line indicates the median, the boxplot limits the 1st and 3rd quartiles and the whiskers' length is 1.5 times the interquartile range.

Naturally, this global rising of groundwater due to climate change does not prevent the occurrence of a depletion in numerous regions. The map on Fig.3.A represents the relative difference of WTD between present-day climate $(1985-2014)$ and the end of the 21st century $(2071-2100)$, following the SSP370 scenario. For readability reasons, we chose to highlight a single scenario (see Supporting Information Fig.$S4$ for the other scenarios). We picked the SSP370 because it is one of the scenarios, along with SSP245, which best match the recent evolution of anthropogenic global fossil-fuel concentrations (Hausfather & Peters, 2020). Despite a global WTD rising of 3.8[3.6-4.0]%, these results show a clear North-South dipole in Europe and America between groundwater rising in the north and depletion in the south (north of the 45° latitude, approximately). The Mediterranean basin, Southern Africa, Amazonia, central America, Australia and parts of China should experience a strong groundwater depletion, whilst central Africa, India, Indonesia and eastern Argentina should see an increase of their groundwater resources with climate change. This spatial pattern

of the WTD changes are the same for all scenarios, the severity of which only impacts the amplitude of the changes and not their sign.

Overall, our projections of groundwater levels are consistent with the findings of the few previous studies based on CMIP5 scenarios which addressed the question of future groundwater resources at the global scale, using a fully coupled model (Wu et al., 2020) or global hydrological models run offline (Reinecke et al., 2021).

3.2 Climate drivers of the WTD changes

Almost everywhere, the sign of WTD changes is determined by the changes of precipitation rather than evapotranspiration. Generally, the water table rises if the precipitation increases and vice versa, whereas an increase (respectively decrease) of evapotranspiration rarely leads to a depletion (rise) of the aquifer (Fig.3). To further investigate this matter, two linear regression models were computed for each grid point: the first one links the 5-yr running mean time-series of WTD with precipitation, and the second one also accounts for the evapotranspiration time-series. The comparison of the corresponding R-squared (Fig.4) shows that over most regions, the second regression model is only slightly better than the first one, given that the correlation between WTD and precipitation is already very high (R-squared over 0.8) and that evapotranspiration is also highly correlated to precipitation. In most places therefore, precipitation proves to be the main driver of the WTD long-term evolution, hence the widespread agreement of signs between the trends of WTD and precipitation (blue and red areas on Fig.3.D).

There are however a few regions where the inclusion of evapotranspiration in the regression model considerably improves the rather low R-squared obtained with precipitation only (Fig.4), which means that evapotranspiration then plays a major role in the evolution of WTD. This is consistent with previous studies (Condon et al., 2020; Wu et al., 2020) which stressed the importance of evapotranspiration in the future evolution of groundwater. The regions where the influence of evapotranspiration prevails correspond to the areas of disagreement between the precipitation and WTD changes (orange and green areas on Fig.3.D), which are in fact characterized by a lack of significance on the precipitation changes (Fig.3.B). In these cases, either the water table deepens with the increase of evapotranspiration (green areas on Fig.3.D) or it rises with the reduction of evapotranspiration (orange areas on Fig.3.D). It is easy to understand how evapotranspiration can increase in a warmer climate. But the decrease of evapotranspiration, in the absence of a significant change of precipitation, is somewhat surprising. Further analysis shows that it is explained by land use change features in SSP scenarios (Hurtt et al., 2020) imposed on the CNRM-ESM2-1 model. For example, the deforestation of the Congo Basin in the SSP370 scenario favours groundwater recharge, as it reduces the withdrawal of soil moisture for deep rooted trees transpiration. Indeed, the conversion of forest to agricultural lands can cause an increase in groundwater recharge even if rainfall slightly decreases (Owuor et al., 2016).

Our analysis of the drivers of WTD changes concerns the aquifers shallower than 100 meters in the world's major groundwater basins, which altogether cover 40% of the land surface. However, it is reasonable to assume that aquifers which are not represented in the CNRM models will be driven by the same climate variables (i.e precipitation and evapotranspiration when precipitation changes are not statically significant). Thus, it seems reasonable to assume that the evolution of the non-represented groundwater basins will mainly follow the precipitation and the evapotranspiration changes.
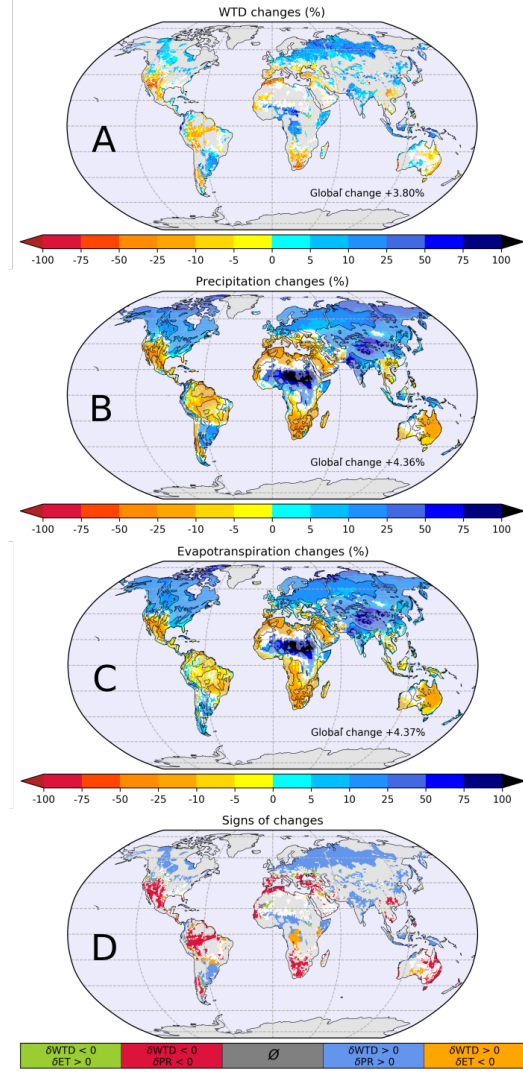
Figure 3. Water Table Depth (**A**), Precipitation (**B**) and Evapotranspiration (**C**) changes (in %) between $1985 - 2014$ in the historical experiment and $2071 - 2100$ in the SSP370 scenario (the values of the change averaged over land are annotated on the maps). Areas in blue (red) correspond to a future WTD rise (depletion) (**A**) or an increase (decrease) of precipitation/evapotranspiration (**B/C**). The white regions correspond to areas where the changes are not statistically significant according to the FDR test (Wilks, 2006, 2016) at a 95% level of confidence. On **B** and **C**, the localisation of the groundwater basins is emphasized to facilitate the comparison with WTD (**A**). **D**: in red and blue : comparison of the sign of WTD and precipitation (PR) changes ; in yellow and green : comparison of the sign of WTD and evapotranspiration (ET) changes wherever the sign of precipitation changes is not consistent with the sign of WTD changes. The white regions correspond to areas where WTD changes are not statistically significant.

3.3 Multi-model analysis

To further explore the uncertainties on the groundwater response to climate change in the CMIP6 experiments, it would be necessary to conduct a multi-model analysis. Unfortunately, in the CMIP6 cohort, the CNRM models are ones of the few which compute
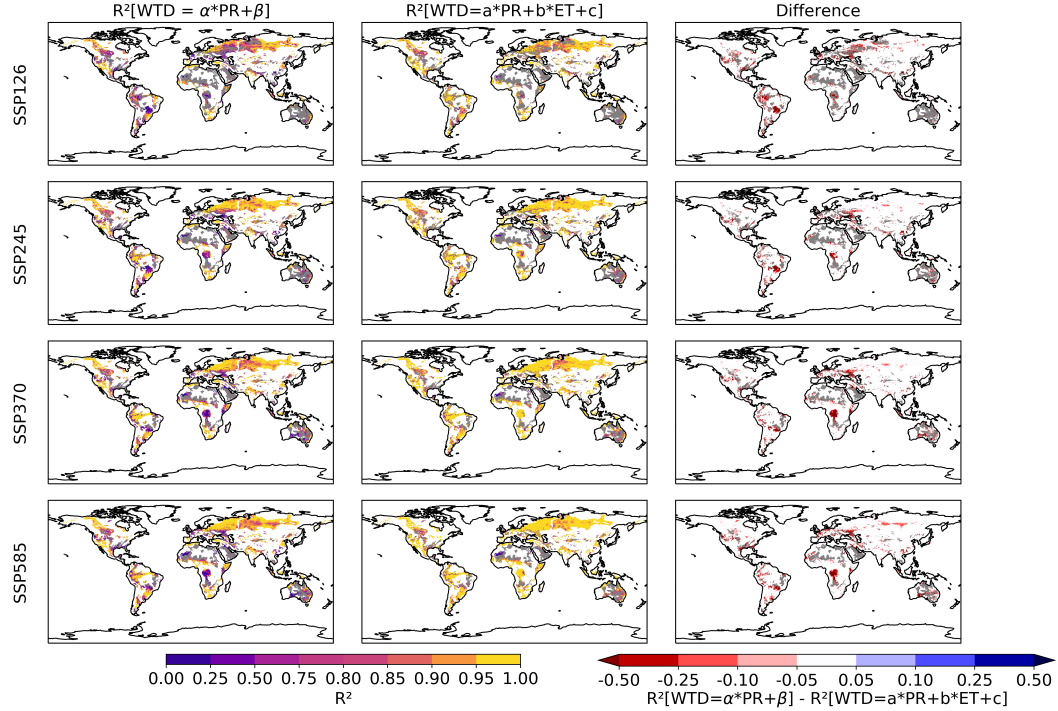
Figure 4. Left panel: R² values of the linear regressions for the statistical model $WTD = \alpha * PR + \beta$. The linear regression is computed for each grid point with samples made of the yearly mean values of each variables for each SSP scenarios (i.e. all years from 2014 to 2100). Center panel: Same as left panel but for the statistical model $WTD = a * PR + b * ET + c$. Right panel: R² values differences between the second model (center panel) and the first one (left panel). Red areas correspond to areas where WTD changes are better correlated with both precipitation and evapotranspiration changes than with precipitation changes only.

water table depth, but the only one using an hydrogeological modelling approach. The question can not therefore be addressed directly. We can however confront the CNRM models' projections of precipitation and evapotransporation to those simulated by 18 other state-of-the-art climate models contributing to CMIP6. Given that these two climate variables drive the long-term trends of WTD, they are responsible for a significant part of the uncertainties associated with the projections of WTD.

Results of this multi-model analysis show that overall, the CNRM models agree with the other CMIP6 models on the evolution of precipitation and evapotranspiration over land surfaces in the future (Fig.5 and Fig.6). The CNRM models global time-series (1850-2100) fall within the range of the inter-model spread. The spatial patterns of precipitation and evapotranspiration future changes of the CNRM models are also in agreement with the CMIP6 multi-model ensemble results (Fig.7). This naturally reflects the findings already reported in the AR6 (IPCC, 2021a), as well as in the previous IPCC assessment report (IPCC, 2013b). In both cases (CNRM models and CMIP6 ensemble), the future climate is projected to be wetter and more humid in most regions outside of the Mediterranean, Australia, southern Africa, Brazil and Central America. The few areas where the CNRM models results disagree with the CMIP6 multi-model mean on the sign of the changes correspond to transition zones between regions of humidification and drying. And in most of these places, the climate change signal is not statistically significant in the CNRM models.
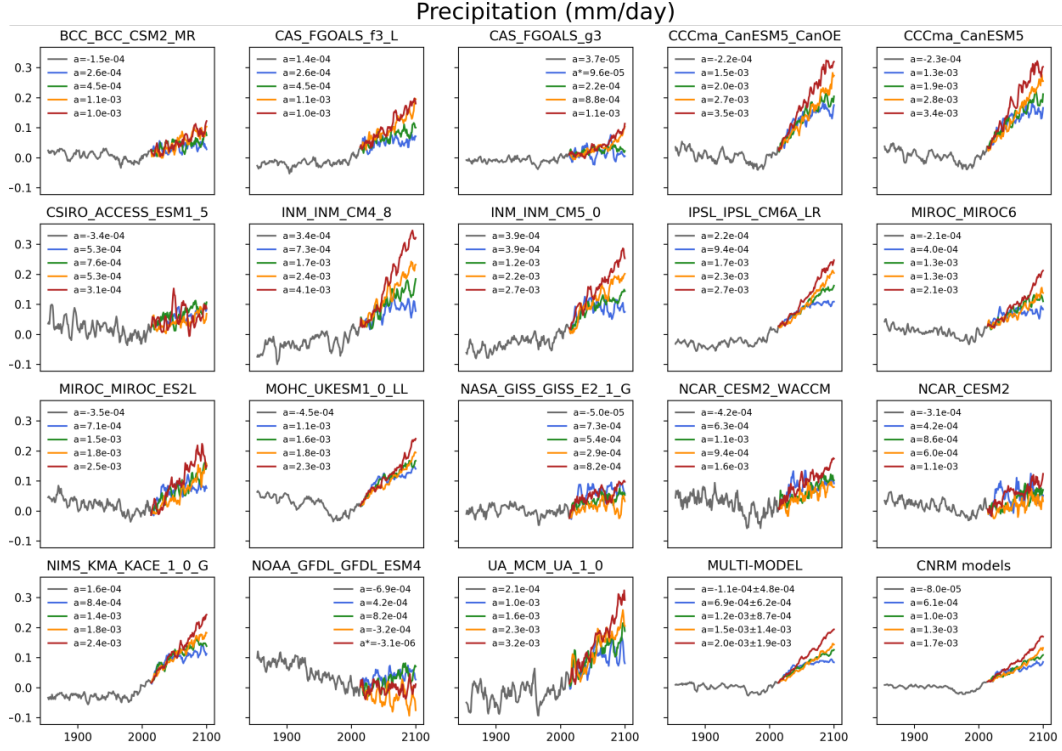
Figure 5. Times-series $(1850 - 2100)$ of the 5-yr running means of global land precipitation anomalies (relatively to $1985 - 2014$) for each SSP scenario: ensemble means of the model references in Table1 to the exclusion of the CNRM models, multi-model ensemble of these ensemble means, and ensemble mean of the CNRM models. a is the slope of the linear regression of each time-series. $a*$ indicates that the slope is not significantly different from 0. The range of the inter-model spread for linear trend of the multi-model ensemble is also given.

³⁴⁶ This agreement between the CNRM models and the CMIP6 multi-model ensembles regard-
³⁴⁷ ing the climatic drivers of WTD changes provides an increased confidence in our projections
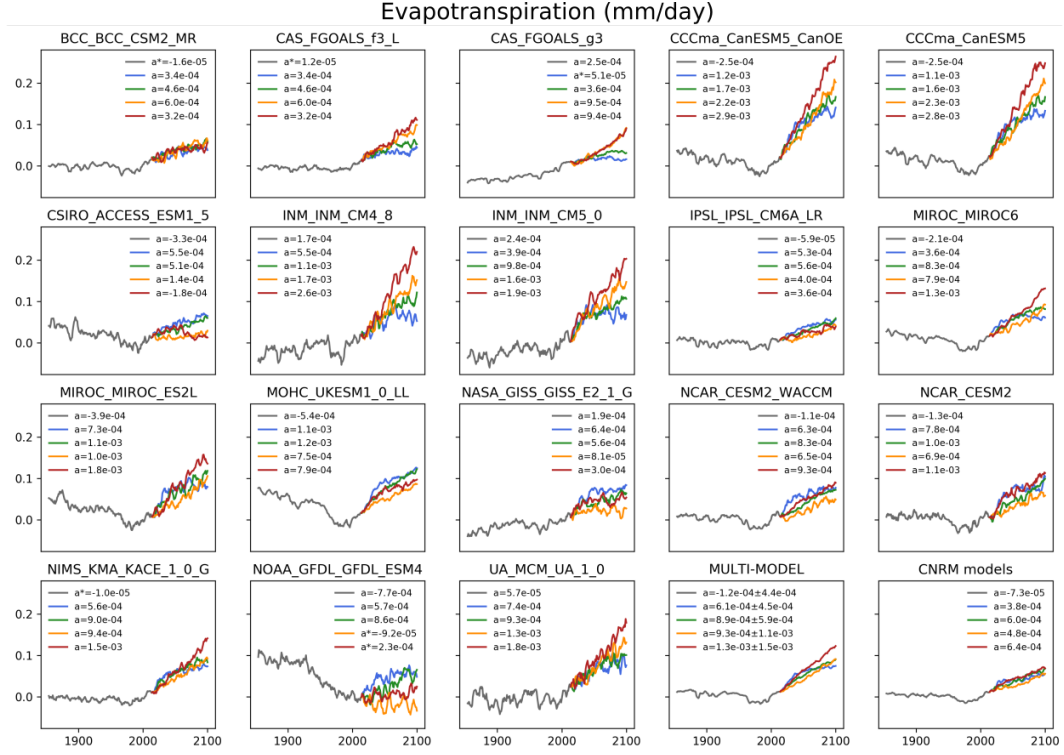³⁴⁸ of groundwater levels.

Figure 6. Same as Fig.5 but for evapotranspiration.

3.4 Potential humans impacts in 2100

Our projections of future groundwater levels can also be analysed in terms of the foreseeable impact on human water risks. To perform the said analysis, we used projections of population densities in 2100 (Supporting Information Fig.$S2$), which we derived from the current population density (2015) provided by the SocioEconomic Data and Applications Center(SEDAC, 2018) and the projected relative changes of population in each country, provided for each SSP scenario(KC & Lutz, 2017). The goal is to determine how the population might be impacted by the variation of WTD with climate change.

Because human withdrawals of groundwater are not represented in the CNRM models, our projections of WTD might be somewhat biased, in the sense that some of the simulated future water tables might be shallower than they would be with the inclusion of groundwater pumping. Indeed, it has been shown that pumping can cause or worsen the depletion of aquifer basins(IPCC, 2021a, 2022b; Famiglietti, 2014; Doll et al., 2009; Gurdak, 2017; Scanlon et al., 2012; Wu et al., 2020). Irrigation accounts for 70% of groundwater withdrawals (Siebert et al., 2010) and thus constitutes the main use of groundwater. Using maps of areas currently equipped for irrigation (see Supporting Information Fig $S3$) we find that 2.8% of the areas located over large groundwater basins are equipped for irrigation and 0.9% specifically for groundwater irrigation. By 2100, most of the future scenarios of global irrigated areas show either a stagnation of irrigated areas or a slight increase followed by a decrease. In the few scenarios projecting an increase of the global irrigated area, its future extent does not exceed twice the present-day values computed over the historical period (Hurtt et al., 2020). Thus, groundwater irrigation should still affect only a small portion of the land surface, which suggests that in most parts of the world, our climate driven-estimates should not be biased by the lack of groundwater irrigation in the CNRM models.
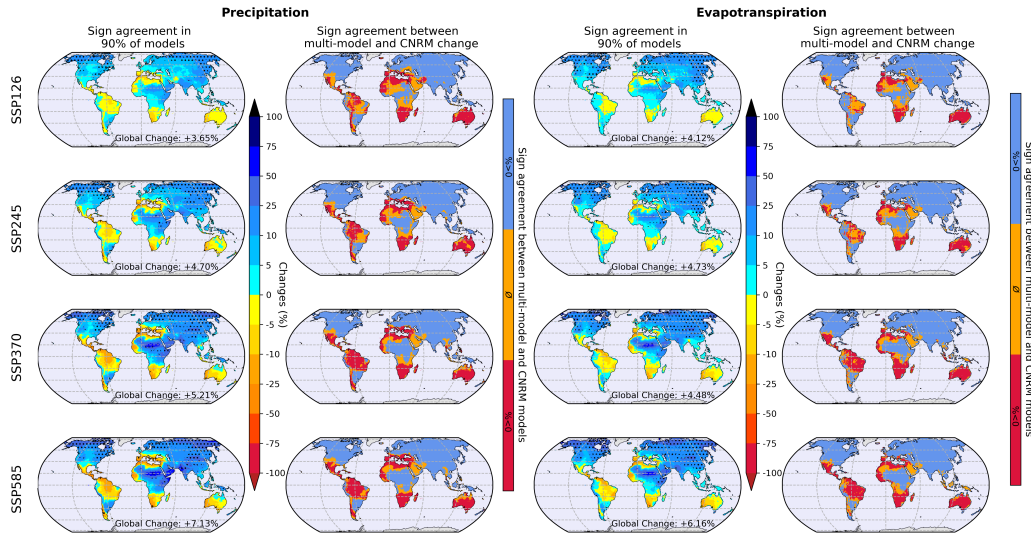
Figure 7. First column: Multi-model ensemble (excluding the CNRM models) of precipitation relative change (in %) between $1985 - 2014$ and $2071 - 2100$ for each SSP scenario. Black dots indicate areas where 90% of the models agree on the sign of the change. Second column: Comparison of the precipitation multi-model change with the change simulated by the CNRM models. In blue: common increase ; in red: common decrease ; in orange: opposite signs of change. Third and fourth columns: same as the first and second columns but for evapotranspiration.

In the following, we further discuss this point using the future population density. Indeed, the comparison of areas currently equipped for irrigation with the word's population density (see Fig.$S3$ and Fig.$S1$ in Supporting Information) shows that except in the US great plains, irrigated areas are densely populated, while the reverse is not necessarily true. Future population density therefore allows to determine where groundwater irrigation could actually matter and also integrates other uses of groundwater (domestic and industrial uses).

Figures 8 and 9 gather the information on WTD and population density in 2100. If we consider the area covered by the world's major groundwater basins we studied here, we find that 40[34-47]% to 52[50-54]% (respectively 20[19-24]% to 26[25-29]%) of this surface will be affected by a rise (respectively a depletion) of groundwater levels (Fig.8). In terms of population, the global pie chart on Fig.9 indicates that, for the SSP370 scenario, 49% of the world's population in 2100 is projected to live in regions located above large groundwater basins and is therefore likely to rely on groundwater resources (see Supporting Information Fig.$S6$ for the other scenarios). Among them, 18[17-19]% ($\sim 1.1[1.0-1.1]$ billion people) are projected to be affected by groundwater depletion, 67[67-71]% ($\sim 4.0[4.0-4.2]$ billion people) by a rising of groundwater levels, and 14[11-15]% would experience no significant change. People living outside these large groundwater basins could however still partly rely on groundwater resources, either because they live near a large aquifer or because they exploit more localised aquifers. Considering all land surfaces (i.e. whether or not they are located above large groundwater basins) in each of the regions defined on Figure 9, we find that 16% of the world's population (~ 2.0 billion people) is projected to live in regions where climate change mostly induces a decline of future groundwater resources, such as the Mediterranean region or northwest America. For the 84% of people (~ 10.2 billion people) living in regions where aquifer levels are mostly projected to rise, the increase of groundwater resources could be lessened by human withdrawals, or even reverse into a decrease in the more highly populated areas, such as South Asia. Note that the computation of confi-
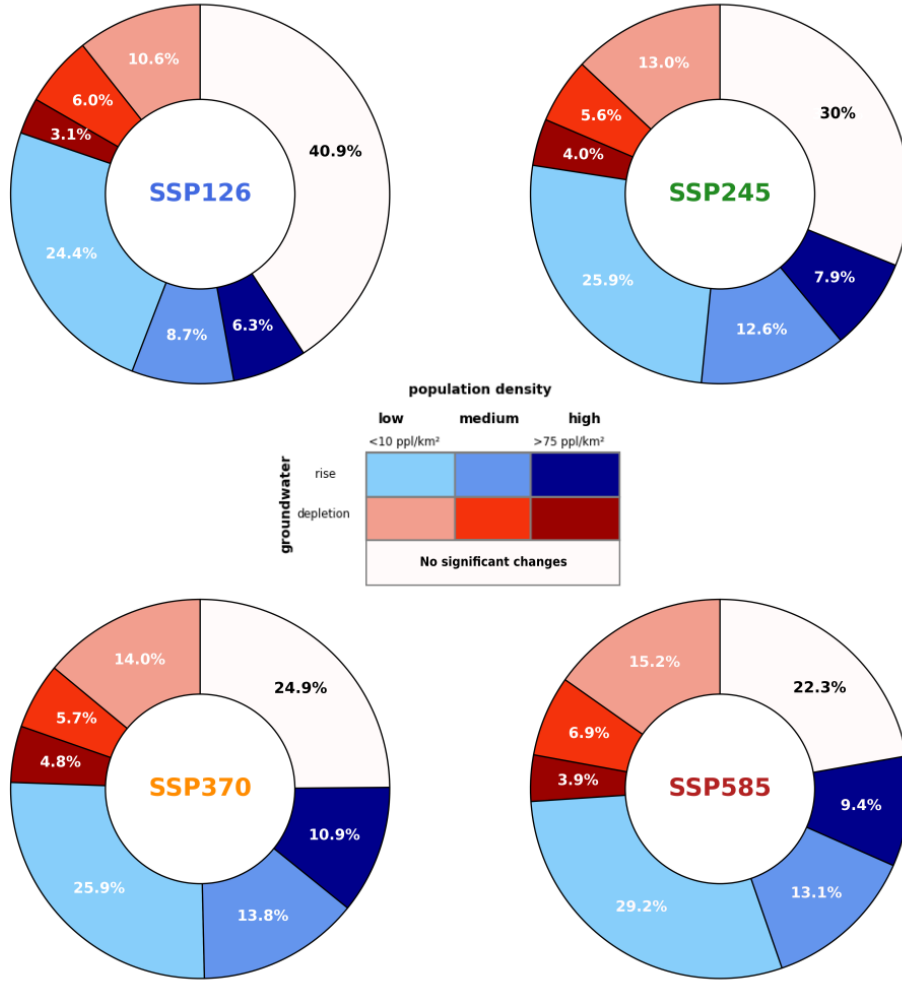
Figure 8. Share of area covered by the world's major groundwater basins where groundwater levels are projected to rise (blue) and to deplete (red). The color intensity indicates the projected population density (people per km^2) in 2100. The light colours correspond to areas with fewer than 10 inhabitants per square kilometer and the dark colours to areas with more than 75 inhabitants per square kilometer. The white regions correspond to areas where WTD changes between $1985 - 2014$ and $2071 - 2100$ are not statistically significant.

dence intervals does not apply in these two cases, as we consider the dominant sign of WTD changes over large regions and it remains the same throughout the bootstrap resampling of our ensemble of simulations.

In all scenarios, the areas currently equipped for groundwater irrigation amount to $\sim 1\%$ of the surface where WTD are projected to rise and 0.5% to 0.8% of the surface where the changes of WTD are not statistically significant in our projections (see table on Fig.$S5$ in Supporting Information). So while the inclusion of human withdrawals would locally reverse the sign of our projections of WTD changes, it would have little effect on the percentages of area and population affected by a rise or depletion of groundwater, therefore not invalidating the figures we gave in the previous paragraph.
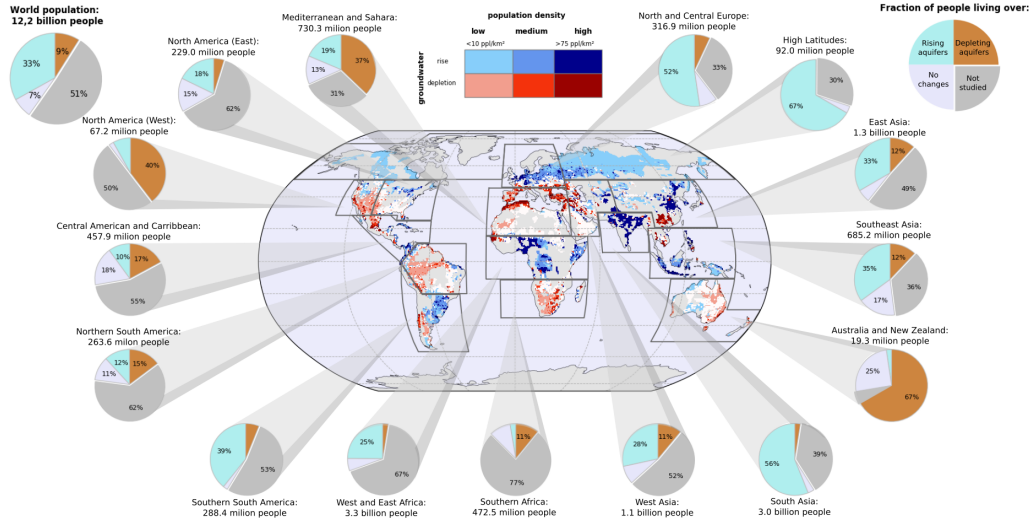
Figure 9. Evolution of WTD and population density in 2100 with the SSP370 scenario. As in Fig.8, aquifer areas are coloured blue (red) if groundwater levels are projected to rise (deepen), whilst the color intensity indicates the projected population density in 2100. The global pie chart (left hand corner) represents the distribution of the world's population which could be affected by a rising (turquoise) or a depletion (brown) of groundwater levels, or which is likely to live above an aquifer basin where future changes are not significant (white) or over unstudied areas (grey). The same pie charts are given for each selected region, defined as those used in the Atlas of Global and Regional Climate Projections in the Annex 1 of the IPCC AR5 (IPCC, 2013a).

We now consider the water risks associated with WTD changes. Three different types of situations can be identified. The first one corresponds to moderately populated areas where aquifers are projected to rise, such as the high latitudes or parts of Northern Europe. In these regions, water stress should not be an issue in the future, as the risk of human withdrawal exceeding the projected increase of groundwater storage can be considered as moderate. There could however be an increased flood risk. Indeed, the saturation of aquifers and overlaying soils can foster or worsen spring freshets and floods associated with periods of intense precipitation.

The second case corresponds to highly populated areas such as South Asia or central Africa, where groundwater levels are also projected to rise. The flood risk might increase in these regions, as in those previously mentioned. With a high population density however, human water requirements are expected to be significant and even increase with climate change and/or the growth of the population. The projected increase of groundwater storage could therefore be reversed and become a decrease, as is already the case in the Ganges valley in North India and in North China where groundwater is already depleted (Rodell et al., 2009; Siebert et al., 2010; Panda et al., 2021). The projected increase of precipitation with climate change could either lead to a replenishment and further increase of groundwater resources in these regions (albeit less than projected in our simulations) or it could be entirely compensated, and even surpassed, by a growing human strain on groundwater.

The third situation corresponds to regions such as the Mediterranean, southern Africa and southwestern USA. In these moderately to highly populated places, the mean regional WTD is projected to deepen, corresponding to a depletion of groundwater (even without taking into account human withdrawal). This could be a huge problem in populated areas

where the drop of WTD will widen the risk of water stress, especially in regions that are already groundwater-dependant(Iglesias et al., 2007) such as the central valley in California. Again, in these regions, the real future depletion should be much stronger than projected, as human withdrawals are not taken into account in the CNRM models and are likely to increase in the future..

4 Summary and prospect

The CNRM models provide a spatially contrasted response of groundwater to climate change throughout the 21st century. In all scenarios, the area experiencing a rise in groundwater levels (39[34-47]% to 52[49-54]% depending on the scenario) is twice the area experiencing a depletion (20[19-24]% to 25[25-29]%). Discussing the potential water risks associated with this projected evolution of groundwater levels, we find that depending on the scenario, 0.7[0.6-0.7] to 1.1[1.1-1.1] billion people (9[9-11]% of the world's population in SSP126 to 9[9-9]% of the world's population in SSP370) could be affected by groundwater depletion in 2100 and thus face water scarcity issues. On the contrary, 1.4[1.3-1.7] to 4.0[4.0-4.3] billion people (21[20-25]% of the world's population in SSP126 to 33[33-35]% of the world's population in SSP370) could see their groundwater resources increase, but this could come at the cost of a higher risk of flood events and landslides, due to the seasonal or occasional saturation of aquifers. The confidence in our estimates of the long-term climate driven-evolution of groundwater level is increased by the agreement between our projections of the main climatic drivers of this evolution (precipitation and evapotranspiration) and CMIP6 multi-model ensemble projections of these drivers.

Nonetheless, to further assess the uncertainties on the groundwater response to future climate change, we argue in favor of a more comprehensive multi-model approach, which would rely on coupled global climate models or Earth system models including a realistic representation of groundwater processes. Other members of the climate and/or hydrology modelling communities have also advocated for the development and use of such holistic global models(Fan et al., 2013; Clark et al., 2015; Boe, 2021; Gleeson et al., 2021). Improving and increasing our confidence in the projections of future groundwater resources does indeed constitute a high-stake issue because it conditions the implementation of suitable mitigation and adaptation plans to counter the widening risks of water scarcity(Famiglietti, 2014; Thomas & Famiglietti, 2019).

Beyond the necessity to account for a valuable representation of groundwater processes in global climate models, we emphasize the need to consider the representation of groundwater pumping and irrigation processes (groundwater contributes to 42% of irrigated water(Doll et al., 2012), which amounts to 70% of human groundwater intake(Siebert et al., 2010)). As we discussed in section 3.4, the consideration of human groundwater withdrawal and its future evolution is likely to locally modulate, and in some places even invert, the impact of the future climate change on groundwater(Wada, 2016; Wu et al., 2020). This modulation of the groundwater evolution, along with the modification of evapotranspiration and/or hydrological processes induced by irrigation, could affect in return the projected climate, hence the need to include these processes in fully coupled climate models.

5 Open Research

All the CNRM climate models and multi-model ensemble data are freely available on the ESGF website (`https://esgf-node.ipsl.upmc.fr/search/cmip6-ipsl/`). The SEDAC data are available at `https://sedac.ciesin.columbia.edu/data/set/gpw-v4 -population-density-rev11`, the CMIP6 projection of population density by country at `https://tntcat.iiasa.ac.at/SspDb/dsd?Action=htmlpage\&page=30`, the GMTED

1km topography data at `https://topotools.cr.usgs.gov/gmted_viewer/`, the global map of the groundwater resources of the world from WHYMAP at `http://www.whymap.org`, and the the principal aquifers of the conterminous United States from the USGS at `https://water.usgs.gov/GIS/metadata/usgswrd/XML/aquifers_us.xml`. The irrigation datas from FAO are available at `https://data.apps.fao.org/aquamaps/`.

Acknowledgments

References

Alley, W. M., Healy, R. W., LaBaugh, J. W., & Reilly, T. E. (2002). Flow and storage in groundwater systems. *Science*, *296*(5575), 1985–1990. doi: 10.1126/science.1067123

Amanambu, A. C., Obarein, O. A., Mossa, J., Li, L., Ayeni, S. S., Balogun, O., ... Ochege, F. U. (2020). Groundwater system and climate change: Present status and future considerations. *Journal of Hydrology*, *589*(May), 125163. Retrieved from `https://doi.org/10.1016/j.jhydrol.2020.125163` doi: 10.1016/j.jhydrol.2020.125163

Anyah, R. O., Weaver, C. P., Miguez-Macho, G., Fan, Y., & Robock, A. (2008). Incorporating water table dynamics in climate modeling: 3. Simulated groundwater influence on coupled land-atmosphere variability. *Journal of Geophysical Research Atmospheres*, *113*(7). doi: 10.1029/2007JD009087

Boe, J. (2021). The physiological effect of CO2 on the hydrological cycle in summer over Europe and land-atmosphere interactions. *Climatic Change*, *167*(1-2), 1–20. doi: 10.1007/s10584-021-03173-2

Cazenave, A., Dieng, H.-b., Meyssignac, B., Schuckmann, K. V., Decharme, B., & Berthier, E. (2014). The rate of sea-level rise. *Nature Climate Change*, *4*(May), 358–361. doi: 10.1038/NCLIMATE2159

Clark, M. P., Fan, Y., Lawrence, D. M., Adam, J. C., Bolster, D., Gochis, D. J., ... Maxwell, R. M. (2015). Improving the representation of hydrologic processes in Earth SystemModels. *Water Resources Research*, *51*, 5929–5956. doi: 10.1002/2015WR017096.Received

Condon, L. E., Atchley, A. L., & Maxwell, R. M. (2020). Evapotranspiration depletes groundwater under warming over the contiguous United States. *Nature Communications*, *11*(1). Retrieved from `http://dx.doi.org/10.1038/s41467-020-14688-0` doi: 10.1038/s41467-020-14688-0

Decharme, B., Delire, C., Minvielle, M., Colin, J., Vergnes, J. P., Alias, A., ... Voldoire, A. (2019). Recent Changes in the ISBA-CTRIP Land Surface System for Use in the CNRM-CM6 Climate Model and in Global Off-Line Hydrological Applications. *Journal of Advances in Modeling Earth Systems*, *11*(5), 1207–1252. doi: 10.1029/2018MS001545

Delire, C., Seferian, R., Decharme, B., Alkama, R., Calvet, J. C., Carrer, D., ... Tzanos, D. (2020). The Global Land Carbon Cycle Simulated With ISBA-CTRIP: Improvements Over the Last Decade. *Journal of Advances in Modeling Earth Systems*, *12*(9), 1–31. doi: 10.1029/2019MS001886

Doll, P., Fiedler, K., & Zhang, J. (2009). Global-scale analysis of river flow alterations due to water withdrawals and reservoirs. *Hydrology and Earth System Sciences*, *13*(12), 2413–2432. doi: 10.5194/hess-13-2413-2009

Doll, P., Hoffmann-Dobrev, H., Portmann, F. T., Siebert, S., Eicker, A., Rodell, M., ...

Scanlon, B. R. (2012). Impact of water withdrawals from groundwater and surface water on continental water storage variations. *Journal of Geodynamics*, *59-60*, 143–156. Retrieved from `http://dx.doi.org/10.1016/j.jog.2011.05.001` doi: 10 .1016/j.jog.2011.05.001

Douville, H., Ribes, A., Decharme, B., Alkama, R., & Sheffield, J. (2013). Anthropogenic influence on multidecadal changes in reconstructed global evapotranspiration. *Nature Climate Change*, *3*(1), 59–62. Retrieved from `http://dx.doi.org/10.1038/nclimate1632` doi: 10.1038/nclimate1632

Durr, H. H., Meybeck, M., & Durr, S. H. (2005). Lithologic composition of the Earth's continental surfaces derived from a new digital map emphasizing riverine material transfer. *Global Biogeochemical Cycles*, *19*(4), 1–23. doi: 10.1029/2005GB002515

Eyring, V., Bony, S., Meehl, G. A., Senior, C. A., Stevens, B., Stouffer, R. J., & Taylor, K. E. (2016). Overview of the Coupled Model Intercomparison Project Phase 6 (CMIP6) experimental design and organization. *Geoscientific Model Development*, *9*(5), 1937–1958. doi: 10.5194/gmd-9-1937-2016

Famiglietti, J. S. (2014). The global groundwater crisis. *Nature Climate Change*, *4*(11), 945–948. Retrieved from `http://dx.doi.org/10.1038/nclimate2425` doi: 10.1038/nclimate2425

Fan, Y., Clark, M., Lawrence, D. M., Swenson, S., Band, L. E., & Brantley, S. L. (2019). Hillslope Hydrology in Global Change Research and Earth System Modeling Water Resources Research. *Water Resources Research*, *55*, 1737–1772. doi: 10.1029/2018WR023903

Fan, Y., Li, H., & Miguez-Macho, G. (2013). Global patterns of Groundwater Table Depth. *Science*, *339*(6122), 940–943. doi: 10.1126/science.1229881

Gleeson, T., Wagener, T., Doll, P., Zipper, S. C., West, C., Wada, Y., . . . Maxwell, R. (2021). GMD perspective: The quest to improve the evaluation of groundwater representation in continental- to global-scale models. *Geoscientific Model Development*, *14*(April), 7545–7571.

Green, T. R., Taniguchi, M., Kooi, H., Gurdak, J. J., Allen, D. M., Hiscock, K. M., . . . Aureli, A. (2011). Beneath the surface of global change: Impacts of climate change on groundwater. *Journal of Hydrology*, *405*(3-4), 532–560. doi: 10.1016/j.jhydrol.2011 .05.002

Gurdak, J. J. (2017). Climate-induced pumping. *Nature Geoscience*, *10*.

Hausfather, Z., & Peters, G. P. (2020). Emissions – the 'business as usual' story is misleading. *Nature*, *577*(7792), 618–620. doi: 10.1038/d41586-020-00177-3

Hurtt, G. C., Chini, L., Sahajpal, R., Frolking, S., Bodirsky, B. L., Calvin, K., . . . Hasegawa, T. (2020). Harmonization of global land use change and management for the period 850 – 2100 (LUH2) for CMIP6. *Geoscientific Model Development*, *13*, 5425–5464.

Iglesias, A., Garrote, L., Flores, F., & Moneo, M. (2007). Challenges to manage the risk of water scarcity and climate change in the Mediterranean. *Water Resources Management*, *21*(5), 775–788. doi: 10.1007/s11269-006-9111-6

IPCC. (2013a). Annex I: Atlas of Global and Regional Climate Projections [van Oldenborgh, G.J., M. Collins, J. Arblaster, J.H. Christensen, J. Marotzke, S.B. Power, M. Rummukainen and T. Zhou (eds.)]. In: Climate Change 2013: The Physical Sci-ence Basis. Contribution of Working Group I to the Fifth Assessment Report of the Intergovernmental Panel on Climate Change [Stocker, T.F., D. Qin, G.-K. Plattner, M. Tignor, S.K. Allen, J. Boschung, A. Nauels, Y. Xia, V. Bex and P.M. Midgley (eds.)]. Cambridge University Press, Cambridge, United Kingdom and New York, NY, U.

IPCC. (2013b). Climate Change 2013: The Physical Science Basis. Contribution of Working Group I to the Fifth Assessment Report of the Intergovernmental Panel on Climate Change [Stocker, T.F., D. Qin, G.-K. Plattner, M. Tignor, S.K. Allen, J. Boschung, A. Nauels, Y. Xia, V. Bex and P.M. Midgley (eds.)]. Cambridge University Press, Cambridge, United Kingdom and New York, NY, USA, 1535 pp.

IPCC. (2021a). Climate Change 2021: The Physical Science Basis. Contribution of Working Group I to the Sixth Assessment Report of the Intergovernmental Panel on Climate

Change[Masson-Delmotte, V., P. Zhai, A. Pirani, S.L. Connors, C. Péan, S. Berger, N. Caud, Y. Chen, L. Goldfarb, M.I. Gomis, M. Huang, K. Leitzell, E. Lonnoy, J.B.R. Matthews, T.K. Maycock, T. Waterfield, O. Yelekçi, R. Yu,and B. Zhou (eds.)]. Cambridge University Press.In Press.

IPCC. (2021b). Douville, H., K. Raghavan, J. Renwick, R.P. Allan, P.A. Arias, M. Barlow, R. Cerezo-Mota, A. Cherchi, T.Y. Gan, J. Gergis, D. Jiang, A. Khan, W. Pokam Mba, D. Rosenfeld, J. Tierney, and O. Zolina, 2021:Water Cycle Changes. InClimate Change 2021: The Physical Science Basis. Contribution of Working Group I to the Sixth Assessment Report of the Intergovernmental Panel on Climate Change[Masson-Delmotte, V., P. Zhai, A. Pirani, S.L. Connors, C. Péan, S. Berger, N. Caud, Y. Chen, L. Goldfarb, M.I. Gomis, M. Huang, K. Leitzell, E. Lonnoy, J.B.R. Matthews, T.K. Maycock, T. Waterfield, O. Yelekçi, R. Yu, and B. Zhou (eds.)].Cambridge University Press. In Press.

IPCC. (2021c). Lee, J.-Y., J. Marotzke, G. Bala, L. Cao, S. Corti, J.P. Dunne, F. Engelbrecht,E. Fischer, J.C. Fyfe, C. Jones, A. Maycock, J. Mutemi, O. Ndiaye, S. Panickal, and T. Zhou:2021, Future Global Climate: Scenario-Based Projections and Near-Term Information. In Climate Change 2021: The Physical Science Basis. Contribution of Working Group I to the Sixth Assessment Report of the Intergovernmental Panel on Climate Change[Masson-Delmotte, V., P. Zhai, A. Pirani, S.L. Connors, C. Péan, S. Berger, N. Caud, Y. Chen, L. Goldfarb, M.I. Gomis, M. Huang, K. Leitzell, E. Lonnoy, J.B.R. Matthews, T.K. Maycock, T. Waterfield, O. Yelekçi, R. Yu, and B. Zhou (eds.)].Cambridge University Press. In Press.

IPCC. (2022a). Caretta, M.A., A. Mukherji, M. Arfanuzzaman, R.A. Betts, A. Gelfan, Y. Hirabayashi, T.K. Lissner, J. Liu, E. Lopez Gunn, R. Morgan, S. Mwanga, and S. Supratid, 2022: Water. In: Climate Change 2022: Impacts, Adaptation, and Vulnerability. Contribution of Working Group II to the Sixth Assessment Report of the Intergovernmental Panel on Climate Change [H.-O. Pörtner, D.C. Roberts, M. Tignor, E.S. Poloczanska, K. Mintenbeck, A. Alegría, M. Craig, S. Langsdorf, S. Löschke, V. Möller, A. Okem, B. Rama (eds.)]. Cambridge University Press. In Press.

IPCC. (2022b). IPCC, 2022: Climate Change 2022: Impacts, Adaptation, and Vulnerability. Contribution of Working Group II to the Sixth Assessment Report of the Intergovernmental Panel on Climate Change [H.-O. Pörtner, D.C. Roberts, M. Tignor, E.S. Poloczanska, K. Mintenbeck, A. Alegría, M. Craig, S. Langsdorf, S. Löschke, V. Möller, A. Okem, B. Rama (eds.)]. Cambridge University Press. In Press.

Kay, J. E., Deser, C., Phillips, A., Mai, A., Hannay, A., Strand, G., . . . Verstenstein, M. (2015). The Community Earth System Model (CESM) Large Ensemble Project: a community resource for studying climate change in the presence of internal climate variability. *Bulletin of the American Meteorological Society*, *96* (August), 1333–1350. doi: 10.1175/BAMS-D-13-00255.1

KC, S., & Lutz, W. (2017). The human core of the shared socioeconomic pathways: Population scenarios by age, sex and level of education for all countries to 2100. *Global Environmental Change*, *42*, 181–192. Retrieved from `http://dx.doi.org/10.1016/j.gloenvcha.2014.06.004` doi: 10.1016/j.gloenvcha.2014.06.004

Larsen, M. A. D., Christensen, J. H., Drews, M., & Butts, M. B. (2016). Local control on precipitation in a fully coupled climate-hydrology model. *Nature Publishing Group* (April). Retrieved from `http://dx.doi.org/10.1038/srep22927` doi: 10.1038/srep22927

Ledoux, E., Girard, G., & De Marsily, G. (1989). Spatially distributed modelling: conceptual approach, coupling surface water and groundwater, in: Unsaturated Flow in Hydrologic Modeling: Theory and Practice. *edited by: Morel-Seytoux, H. J.*, 435-454.

Maxwell, R. M., & Kollet, S. J. (2008). Interdependence of groundwater dynamics and land-energy feedbacks under climate change. *Nature Geoscience*, *1* (10), 665–669. doi: 10.1038/ngeo315

Meinshausen, M., Vogel, E., Nauels, A., Lorbacher, K., Meinshausen, N., Etheridge, D. M., . . . Weiss, R. (2017). Historical greenhouse gas concentrations for climate modelling (CMIP6). *Geoscientific Model Development*, *10* (5), 2057–2116. doi: 10.5194/gmd-10

-2057-2017

Meixner, T., Manning, A. H., Stonestrom, D. A., Allen, D. M., Ajami, H., Blasch, K. W., . . . Walvoord, M. A. (2016). Implications of projected climate change for groundwater recharge in the western United States. *Journal of Hydrology*, *534*, 124–138. Retrieved from `http://dx.doi.org/10.1016/j.jhydrol.2015.12.027` doi: 10.1016/j.jhydrol .2015.12.027

O'Neill, B. C., Kriegler, E., Ebi, K. L., Kemp-Benedict, E., Riahi, K., Rothman, D. S., . . . Solecki, W. (2017). The roads ahead: Narratives for shared socioeconomic pathways describing world futures in the 21st century. *Global Environmental Change*, *42*, 169–180. Retrieved from `http://dx.doi.org/10.1016/j.gloenvcha.2015.01.004` doi: 10.1016/j.gloenvcha.2015.01.004

O'Neill, B. C., Tebaldi, C., Van Vuuren, D. P., Eyring, V., Friedlingstein, P., Hurtt, G., . . . Sanderson, B. M. (2016). The Scenario Model Intercomparison Project (ScenarioMIP) for CMIP6. *Geoscientific Model Development*, *9*(9), 3461–3482. doi: 10.5194/gmd-9 -3461-2016

Owuor, S. O., Butterbach-Bahl, K., Guzha, A. C., Rufino, M. C., Pelster, D. E., Diaz-Pines, E., & Breuer, L. (2016). Groundwater recharge rates and surface runoff response to land use and land cover changes in semi-arid environments. *Ecological Processes*, *5*(1). Retrieved from `http://dx.doi.org/10.1186/s13717-016-0060-6` doi: 10.1186/ s13717-016-0060-6

Padron, R. S., Gudmundsson, L., Decharme, B., Ducharne, A., Lawrence, D. M., Mao, J., . . . Seneviratne, S. I. (2020). Observed changes in dry-season water availability attributed to human-induced climate change. *Nature Geoscience*, *13*(July), 447–481. Retrieved from `http://dx.doi.org/10.1038/s41561-020-0594-1` doi: 10.1038/ s41561-020-0594-1

Panda, D. K., Ambast, S. K., & Shamsudduha, M. (2021). Groundwater depletion in northern India: Impacts of the sub-regional anthropogenic land-use, socio-politics and changing climate. *Hydrological Processes*, *35*(2), 1–16. doi: 10.1002/hyp.14003

Reinecke, R., Schmied, H. M., Trautmann, T., Andersen, L. S., Burek, P., Florke, M., . . . Pokhrel, Y. (2021). Uncertainty of simulated groundwater recharge at different global warming levels : a global-scale multi-model ensemble study. *Hydrology and Earth System Sciences*, *25*, 787–810.

Rodell, M., Velicogna, I., & Famiglietti, J. S. (2009). Satellite-based estimates of groundwater depletion in India. *Nature*, *460*(7258), 999–1002. Retrieved from `http:// dx.doi.org/10.1038/nature08238` doi: 10.1038/nature08238

Roehrig, R., Beau, I., Saint-Martin, D., Alias, A., Decharme, B., Gueremy, J. F., . . . Senesi, S. (2020). The CNRM Global Atmosphere Model ARPEGE-Climat 6.3: Description and Evaluation. *Journal of Advances in Modeling Earth Systems*, *12*(7), 1–53. doi: 10.1029/2020MS002075

Scanlon, B. R., Faunt, C. C., Longuevergne, L., Reedy, R. C., Alley, W. M., McGuire, V. L., & McMahon, P. B. (2012). Groundwater depletion and sustainability of irrigation in the US High Plains and Central Valley. *Proceedings of the National Academy of Sciences of the United States of America*, *109*(24), 9320–9325. doi: 10.1073/pnas .1200311109

Scanlon, B. R., Keese, K. E., Flint, A. L., Flint, L. E., Gaye, C. B., Edmunds, W. M., & Simmers, I. (2006). Global synthesis of groundwater recharge in semiarid and arid regions. *Hydrological Processes*, *20*(15), 3335–3370. doi: 10.1002/hyp.6335

SEDAC. (2018). Center for International Earth Science Information Network - CIESIN - Columbia University. 2018. Gridded Population of the World, Version 4 (GPWv4): Population Density, Revision 11. Palisades, NY: NASA Socioeconomic Data and Applications Center (SEDAC). https://doi.org/10.7927/H49C6VHW. Accessed 18/03/21.

Seferian, R., Nabat, P., Michou, M., Saint-Martin, D., Voldoire, A., Colin, J., . . . Madec, G. (2019). Evaluation of CNRM Earth System Model, CNRM-ESM2-1: Role of Earth System Processes in Present-Day and Future Climate. *Journal of Advances in Modeling Earth Systems*, *11*(12), 4182–4227. doi: 10.1029/2019MS001791

Siebert, S., Burke, J., Faures, J. M., Frenken, K., Hoogeveen, J., Doll, P., & Portmann, F. T. (2010). Groundwater use for irrigation - A global inventory. *Hydrology and Earth System Sciences*, *14*(10), 1863–1880. doi: 10.5194/hess-14-1863-2010

Taylor, K. E., Stouffer, R. J., & Meehl, G. A. (2012). An Overview of CMIP5 and the experiment design. *Amer. Meteor. Soc.*, *93*, 1333–1349. doi: 10.1175/BAMS-D-11-00094.1

Taylor, R. G., Scanlon, B., Döll, P., Rodell, M., Van Beek, R., Wada, Y., ... Treidel, H. (2013). Ground water and climate change. *Nature Climate Change*, *3*(4), 322–329. doi: 10.1038/nclimate1744

Thomas, B. F., & Famiglietti, J. S. (2019). Identifying Climate-Induced Groundwater Depletion in GRACE Observations. *Scientific Reports*, *9*(1), 1–9. Retrieved from http://dx.doi.org/10.1038/s41598-019-40155-y

Vergnes, J.-P. (May 2014). Développement d'une modélisation hydrologique incluant la représentation des aquifères : évaluation sur la France et à l'échelle globale. *PhD thesis (Institut National Polytechnique de Toulouse)*.

Vergnes, J. P., & Decharme, B. (2012). A simple groundwater scheme in the TRIP river routing model: Global off-line evaluation against GRACE terrestrial water storage estimates and observed river discharges. *Hydrology and Earth System Sciences*, *16*(10), 3889–3908. doi: 10.5194/hess-16-3889-2012

Vergnes, J. P., Decharme, B., Alkama, R., Martin, E., Habets, F., & Douville, H. (2012). A simple groundwater scheme for hydrological and climate applications: Description and offline evaluation over France. *Journal of Hydrometeorology*, *13*(4), 1149–1171. doi: 10.1175/JHM-D-11-0149.1

Vergnes J.P., Decharme B, H. F. (2014). Introduction of groundwater capillary rises using subgrid spatial variability of topography into the ISBA land surface model. *Journal of Geophysical Research*(119), 11,065–11,086. doi: 10.1002/2014JD021573.Received

Voldoire, A., Saint-Martin, D., Senesi, S., Decharme, B., Alias, A., Chevallier, M., ... Waldman, R. (2019). Evaluation of CMIP6 DECK Experiments With CNRM-CM6-1. *Journal of Advances in Modeling Earth Systems*, *11*(7), 2177–2213. doi: 10.1029/2019MS001683

Wada, Y. (2016). Impacts of Groundwater Pumping on Regional and Global Water Resources. *Terrestrial Water Cycle and Climate Change*(May 2016), 337. doi: 10.1007/978-3-319-32449-4

Wada, Y., Van Beek, L. P., Sperna Weiland, F. C., Chao, B. F., Wu, Y. H., & Bierkens, M. F. (2012). Past and future contribution of global groundwater depletion to sea-level rise. *Geophysical Research Letters*, *39*(9), 1–6. doi: 10.1029/2012GL051230

Wang, F., Ducharne, A., Cheruy, F., Lo, M. H., & Grandpeix, J. Y. (2018). Impact of a shallow groundwater table on the global water cycle in the IPSL land–atmosphere coupled model. *Climate Dynamics*, *50*, 3505–3522. Retrieved from http://link.springer.com/10.1007/s00382-017-3820-9 doi: 10.1007/s00382-017-3820-9

Wild, M. (2012). Enlightening global dimming and brightening. *Bulletin of the American Meteorological Society*, *93*(1), 27–37. doi: 10.1175/BAMS-D-11-00074.1

Wilks, D. S. (2006). On 'field significance' and the False Discovery Rate. *Journal of Applied Meteorology and Climatology*, *45*(9), 1181–1189. doi: 10.1175/JAM2404.1

Wilks, D. S. (2016). 'The stippling shows statistically significant grid points': How research results are routinely overstated and overinterpreted, and what to do about it. *Bulletin of the American Meteorological Society*, *97*(12), 2263–2273. doi: 10.1175/BAMS-D-15-00267.1

Wu, W.-Y., Lo, M.-h., Wada, Y., Famiglietti, J. S., Reager, J. T., Yeh, P. J., ... Yang, Z.-L. (2020). Divergent effects of climate change on future groundwater availability in key mid-latitude aquifers. *Nature Communications*, *11*, 1–9. Retrieved from http://dx.doi.org/10.1038/s41467-020-17581-y doi: 10.1038/s41467-020-17581-y